Wide color gamut LCD with a quantum dot backlight

Zhenyue Luo, Yuan Chen, and Shin-Tson Wu*

CREOL, The College of Optics and Photonics, University of Central Florida, Orlando, Florida 32816, USA
** swu@ucf.edu*

Abstract: We analyze the color performance and system efficiency of three commonly employed liquid crystal display modes with a blue LED-pumped red and green quantum dots (QDs) backlight. Based on the measured QD emission spectra, we can achieve 115% color gamut in CIE 1931 and 140% in CIE 1976 color space, while keeping the same energy efficiency as conventional backlights. Next, we apply multi-objective optimization method to refine the QD emission spectra and find a fundamental tradeoff between display system efficiency and color gamut. This systematic photometric analysis also provides useful guidelines for further optimizing QD backlight design and display system efficiency.

OCIS codes: (250.5230) Photoluminescence; (250.5590) Quantum-well, -wire and -dot devices; (160.2540) Fluorescent and luminescent materials; (330.1715) Color, rendering and metamerism; (230.3720) Liquid-crystal devices.

References and links

1. M. Schadt, "Milestone in the history of field-effect liquid crystal displays and materials," Jpn. J. Appl. Phys. **48**(3), 03B001 (2009).
2. D. Barnes, "LCD or OLED, who wins?" SID Symposium Digest of Technical Papers, **44**, 26–27 (2013).
3. Y. Ukai, "TFT-LCDs as the future leading role in FPD," SID Symposium Digest of Technical Papers, **44**, 28–31 (2013).
4. J. H. Lee, K. H. Park, S. H. Kim, H. C. Choi, B. K. Kim, and Y. S. Yin, "AH-IPS, superb display for mobile device," SID Symposium Digest of Technical Papers, **44**, 32–33 (2013).
5. H. Kikuchi, M. Yokota, Y. Hisakado, H. Yang, and T. Kajiyama, "Polymer-stabilized liquid crystal blue phases," Nat. Mater. **1**(1), 64–68 (2002).
6. K. M. Chen, S. Gauza, H. Xianyu, and S. T. Wu, "Submillisecond gray level response time of a polymer-stabilized blue-phase liquid crystal," J. Display Technol. **6**(2), 49–51 (2010).
7. Y. Chen, J. Yan, J. Sun, S. T. Wu, X. Liang, S. H. Liu, P. J. Hsieh, K. L. Cheng, and J. W. Shiu, "A microsecond-response polymer-stabilized blue phase liquid crystal," Appl. Phys. Lett. **99**(20), 201105 (2011).
8. S. Kobayashi, S. Mikoshiba, and S. Lim, *LCD Backlights* (Wiley, 2009).
9. M. Anandan, "Progress of LED backlights for LCDs," J. Soc. Inf. Disp. **16**(2), 287–310 (2008).
10. G. Harbers, S. J. Bierhuizen, and M. R. Krames, "Performance of high power light emitting diodes in display illumination applications," J. Display Technol. **3**(2), 98–109 (2007).
11. R. Lu, S. Gauza, and S. T. Wu, "LED-lit LCD TVs," Mol. Cryst. Liq. Cryst. **488**(1), 246–259 (2008).
12. R. Lu, Q. Hong, S. T. Wu, K. H. Peng, and H. S. Hsieh, "Quantitative comparison of color performances between IPS and MVA LCDs," J. Display Technol. **2**(4), 319–326 (2006).
13. R. J. Xie, N. Hirosaki, and T. Takeda, "Wide color gamut backlight for liquid crystal displays using three-band phosphor-converted white light-emitting diodes," Appl. Phys. Express **2**, 022401 (2009).
14. B. S. Mashford, M. Stevenson, Z. Popovic, C. Hamilton, Z. Q. Zhou, C. Breen, J. Steckel, V. Bulovic, M. Bawendi, S. Coe-Sullivan, and P. T. Kazlas, "High-efficiency quantum-dot light-emitting devices with enhanced charge injection," Nat. Photonics **7**(5), 407–412 (2013).
15. S. Coe-Sullivan, W. Liu, P. Allen, and J. S. Steckel, "Quantum dots for LED downconversion in display applications," ECS J. Solid State Sci. Technol. **2**(2), R3026–R3030 (2013).
16. S. Kim, S. H. Im, and S. W. Kim, "Performance of light-emitting-diode based on quantum dots," Nanoscale **5**(12), 5205–5214 (2013).
17. J. Lim, W. K. Bae, J. Kwak, S. Lee, C. Lee, and K. Char, "Perspective on synthesis, device structures, and printing processes for quantum dot displays," Opt. Mater. Express **2**(5), 594–628 (2012).
18. Y. Shirasaki, G. J. Supran, M. G. Bawendi, and V. Bulovic, "Emergence of colloidal quantum-dot light-emitting technologies," Nat. Photonics **7**(1), 13–23 (2013).

#195594 - $15.00 USD Received 12 Aug 2013; accepted 10 Oct 2013; published 25 Oct 2013

19. T. Erdem, S. Nizamoglu, X. W. Sun, and H. V. Demir, "A photometric investigation of ultra-efficient LEDs with high color rendering index and high luminous efficacy employing nanocrystal quantum dot luminophores," Opt. Express **18**(1), 340–347 (2010).
20. P. Zhong, G. X. He, and M. H. Zhang, "Optimal spectra of white light-emitting diodes using quantum dot nanophosphors," Opt. Express **20**(8), 9122–9134 (2012).
21. J. S. Steckel, R. Colby, W. Liu, K. Hutchinson, C. Breen, J. Ritter, and S. Coe-Sullivan, "Quantum dot manufacturing requirements for the high volume LCD market," SID Symposium Digest of Technical Papers, **44**, 943–945 (2013).
22. J. Chen, V. Hardev, J. Hartlove, J. Hofler, and E. Lee, "A high-efficiency wide-color-gamut solid-state backlight system for LCDs using quantum dot enhancement film," SID Symposium Digest of Technical Papers, **43**, 895–896 (2012).
23. I. H. Campbell and B. K. Crone, "Efficient, visible organic light-emitting diodes utilizing a single polymer layer doped with quantum dots," Appl. Phys. Lett. **92**(4), 043303 (2008).
24. S. Coe-Sullivan, "Quantum dot developments," Nat. Photonics **3**(6), 315–316 (2009).
25. E. Jang, S. Jun, H. Jang, J. Lim, B. Kim, and Y. Kim, "White-light-emitting diodes with quantum dot color converters for display backlights," Adv. Mater. **22**(28), 3076–3080 (2010).
26. http://hexus.net/tech/news/displays/50621-sonys-triluminos-displays-use-quantum-dot-technology/.
27. J. H. Lee, D. N. Liu, and S. T. Wu, *Introduction to Flat Panel Displays* (Wiley, 2008).
28. J. Morovič, *Color Gamut Mapping* (Wiley, 2008).
29. D. K. Yang and S. T. Wu, *Fundamentals of Liquid Crystal Devices* (Wiley, 2006).
30. M. Schadt and W. Helfrich, "Voltage-depenent optical activity of a twisted nematic liquid crystal," Appl. Phys. Lett. **18**(4), 127–128 (1971).
31. H. Hong, H. Shin, and I. Chung, "In-plane switching technology for liquid crystal display television," J. Display Technol. **3**(4), 361–370 (2007).
32. A. Takeda, S. Kataoka, T. Sasaki, H. Chida, H. Tsuda, K. Ohmuro, T. Sasabayashi, Y. Koike, and K. Okamoto, "A super-high image quality multi-domain vertical alignment LCD by new rubbing-less technology," SID Symposium Digest of Technical Papers, **29**, 1077–1080 (1998).
33. C. A. C. Coello and G. B. Lamont, *Applications of Multi-Objective Evolutionary Algorithms* (World Scientificc, 2004).
34. J. Kennedy and R. Eberhart, "Particle swarm optimization," Proc. IEEE International Conference on Neural Networks IV. pp. 1942–1948 (1995).
35. M. Reyes-Sierra and C. A. C. Coello, "Multi-Objective particle swarm optimizers: a survey of the state-of-the-art," Int. J. Comput. Intell. Res. **2**, 287–308 (2006).

1. Introduction

After half a century of extensive material research and device development, followed by massive investment in advanced manufacturing technology, thin-film-transistor liquid-crystal-display (TFT-LCD) has become the dominant flat panel display technology [1]. Nowadays, LCDs are ubiquitous in our daily lives; their applications range from smartphones, tablets, computers, to large-screen TVs, and data projectors. It seems as though LCD technology has reached a fairly mature stage. Most critical issues, such as viewing angle, contrast ratio, power consumption, have been solved to an acceptable level. Recently, there are heated debates between LCD and organic light emitting diode (OLED) camps [2–4]: who wins? OLED indeed offers superior performances to LCD in faster response time (especially in cold ambient), wider viewing angle, wider color gamut, true black state (in a dark room), thinness, and flexibility. A slow-response LCD causes motion picture image blurs, while narrow color gamut degrades color fidelity. To improve response time, polymer-stabilized blue phase LCDs with submillisecond gray-to-gray response time is emerging [5–7]. To widen color gamut, several new backlight sources have been developed [8–10].

Cold cathode fluorescent lamp (CCFL) was once the most prevalent backlight source, but its color gamut is only ~75% of NTSC (National Television Standard Committee) standard. In order to achieve wider color gamut, higher brightness, and lower power consumption, mercury-free white LED (WLED) has rapidly replaced CCFL as the major backlight source [9–12]. WLED can be divided into single chip and multiple chips. A good example of single-chip WLED is to use a blue InGaN LED to pump yellow phosphor (cerium-doped yttrium aluminum garnet: Ce:YAG). This approach is efficient and cost effective. However, its color gamut is limited and cannot faithfully reproduce the natural colors. To enlarge color gamut, new types of green and red phosphor materials have been developed and multiple phosphors

#195594 - $15.00 USD Received 12 Aug 2013; accepted 10 Oct 2013; published 25 Oct 2013

are mixed together to narrow down the emission bandwidth [13]. Up to now the red phosphor material is still quite limited and the conversion efficiency is not yet satisfactory. On the other hand, multiple-chip WLED uses red, green, and blue LEDs to render white color. It provides excellent color performance and tuning abilities. However, complicated and separated driving circuits are required to compensate the thermal-optic effect, which leads to a higher cost. Besides, the availability of high efficiency green LED remains a challenge.

Recently, quantum dot (QD) LED is emerging as a new backlight source [14–18]. Large scale synthesis of QD materials can now be performed at an affordable cost. Resulting from the size quantization effect, QD LED exhibits several attractive features: high quantum efficiency, broad absorption band, narrow emission linewidth, and controllable emission peak. QD LED has already shown great advantages in general lighting with higher efficacy and better rendering ability [19, 20]. It is also a competitive backlight solution for next-generation LCDs. In particular, their narrow emission spectra lead to vivid colors. More amazingly, the individual emission spectrum can be tuned via optimizing QD size/composition to match the transmission peak of a color filter and to reduce the crosstalk between colors. Several companies are actively engaging into this area, including Nanosys, QD vision, Nanoco, and 3M [21–24]. Recently, Samsung [25] and Sony [26] have demonstrated LCD panels with QD backlight. However, a full investigation and systematic performance analysis of QD display is still lacking.

In this paper, we first evaluate and compare various types of conventional backlight solutions in terms of energy efficiency and color performance. We then optimize the emission spectrum of QD light with multi-objective optimization method. In comparison with conventional backlight solutions, QD backlight offers a wider color gamut (over 115% NTSC in CIE 1931 color space and 140% NTSC in CIE 1976) and higher system efficiency. A fundamental tradeoff between color gamut and system efficiency is explained. This systematic photometric analysis establishes an important guideline for further optimizing QD backlight design.

2. Evaluation of conventional backlight sources

2.1 Evaluation criteria

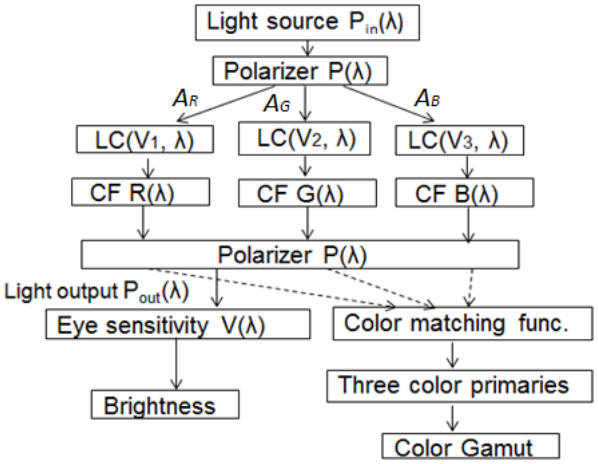

Fig. 1. Light flow chart in a typical LCD system.

For benchmarking, let us first examine the present backlight sources in terms of energy efficiency and color performance. Figure 1 shows the light flow chart in a typical LCD system. Let us assume the light source has a spectral power distribution (SPD) $P_{in}(\lambda)$ and passes through the first polarizer. For simplicity but without losing generality, here we do not

#195594 - $15.00 USD Received 12 Aug 2013; accepted 10 Oct 2013; published 25 Oct 2013

consider other optical elements, such as diffusers, brightness enhancement films, and phase compensation films [8]. The incident light impinges the LCD panel, which consists of TFT array, LC layer, and color filter array, and finally transmits through the crossed analyzer. To analyze the color performance, in Fig. 1 we split the incident light (after polarizer) into three channels: red (R), green (G) and blue (B) corresponding to the color filters. The TFT aperture ratio, LC layer, applied voltage, and color filters jointly determine the optical efficiency and color saturation of a LCD panel. In Fig. 1, we define A_R, A_G and A_B as the aperture ratio of each light channel, and $R(\lambda)$, $G(\lambda)$, and $B(\lambda)$ as the transmission spectra of the color filters. The transmittance of polarizer ($T_{pol}(\lambda)$) is also wavelength dependent; it has a lower transmittance in the blue region due to iodine absorption. Moreover, the transmittance of the LC cell $LC(\lambda,V)$ depends on the wavelength and voltage. Different voltages are applied to each sub-pixel to control the RGB ratios for generating a desired color hue and gray level. From Fig. 1, the SPD of the output light can be written as:

$$\begin{aligned} P_{out}(\lambda) &= P_{out,R}(\lambda) + P_{out,G}(\lambda) + P_{out,B}(\lambda) \\ &= P_{in}(\lambda)P(\lambda)R(\lambda)LC(V_1,\lambda)A_R + P_{in}(\lambda)P(\lambda)G(\lambda)LC(V_1,\lambda)A_G + P_{in}(\lambda)P(\lambda)B(\lambda)LC(V_1,\lambda)A_B, \end{aligned} \quad (1)$$

where $P_{out,R}(\lambda)$, $P_{out,G}(\lambda)$, and $P_{out,B}(\lambda)$ refer to the output SPD for the RGB channels, respectively. As a measure of light spectral efficiency, the luminous efficacy of radiation (LER) [17] is defined as follows:

$$LER = \frac{683\frac{lm}{W_{opt}}\int P_{out}(\lambda)V(\lambda)d\lambda}{\int P_{out}(\lambda)d\lambda}. \quad (2)$$

In Eq. (2), the denominator represents the total radiation power of the output light while the numerator refers to the illuminance that human eye perceives. LER reflects how efficient the output light can be converted to the brightness feeling of human eye. V(λ) is the human eye sensitivity function, it is centered at λ = 550 nm. The maximum value of LER is 683 lm/W_{opt} for a monochromatic light source at λ = 550 nm. However, for a broadband backlight (e.g., white light) its LER is usually much lower.

The second efficiency measure is the transfer efficiency (TE) of the LCD. It is defined as the ratio of transmitted light through the LCD panel over the input light:

$$TE = \frac{\int P_{out}(\lambda)d\lambda}{\int P_{in}(\lambda)d\lambda}. \quad (3)$$

Several parameters can affect TE, such as the absorption loss of polarizers, TFT aperture ratio, LC modulation efficiency, and color filters. Finally, the total light efficiency (TLE) of the display system can be expressed as:

$$TLE = \frac{683\frac{lm}{W_{opt}}\int P_{out}(\lambda)V(\lambda)d\lambda}{\int P_{in}(\lambda)d\lambda} = LER*TE. \quad (4)$$

This value indicates how much input light can be transmitted through the LCD panel and finally be converted to the brightness perceived by human eyes. TLE is a measure of backlight' total efficiency; it considers almost every factor in the display system, such as the efficacy of light source, the transmittance of color filters, LC layer and polarizers, and the aperture ratio of each light channel. The only factor excluded is the wall plug efficiency of the light source itself [10]. But even among the same type of light source, the wall plug efficiency

#195594 - $15.00 USD Received 12 Aug 2013; accepted 10 Oct 2013; published 25 Oct 2013

could be quite different depending on the suppliers. Since our objective is to compare the performance of different backlights for display applications, TLE is a sufficient criterion.

From Eq. (4), backlight's emission spectrum has significant impact on TLE. For example, if the light spectrum is concentrated near 550 nm where human eye is more sensitive, then both LER and TLE would be higher. Also, if the emission spectrum of backlight matches well with the transmission spectrum of color filters, then the system will have higher TE and TLE. A higher TLE implies to higher energy efficiency.

Besides high energy efficiency, LCD backlight display should also have good color rendering. This is mainly determined by the purity of three primary colors. As shown in Fig. 1, red, green and blue lights come out from different channels; their chromaticity coordinates can be calculated based on trichromatic color space theory [27]. The X, Y, Z tristmulus values of a color stimulus S(λ) are expressed as:

$$X = k\int S(\lambda)\bar{x}(\lambda)d\lambda, \qquad Y = k\int S(\lambda)\bar{y}(\lambda)d\lambda, \qquad Z = k\int S(\lambda)\bar{z}(\lambda)d\lambda, \qquad (5)$$

where $\bar{x}(\lambda)$, $\bar{y}(\lambda)$ and $\bar{z}(\lambda)$ represent the three color matching functions and k is a constant. S(λ) equals to $P_{out,R}(\lambda)$, $P_{out,G}(\lambda)$, $P_{out,B}(\lambda)$ respectively when calculating the X, Y, Z tristimulus values for light from RGB channels. The chromaticity coordinates defined in Commission Internationale de l'Elcairage (CIE) 1931 color space is given as:

$$x = \frac{X}{X+Y+Z}, \qquad y = \frac{Y}{X+Y+Z}, \qquad z = \frac{Z}{X+Y+Z}, \qquad (6)$$

while the chromaticity coordinates (u',v') defined in CIE 1976 color space are related to X, Y and Z as:

$$u' = \frac{4X}{X+15Y+3Z}, \qquad v' = \frac{9Y}{X+15Y+3Z}. \qquad (7)$$

Three sets of color coordinates obtained for RGB channels constitute a triangle in the CIE color diagram. All the colors within the triangle can be displayed by a proper mixing of the three color primaries. The area ratio between this triangle and the triangle defined by NTSC is called color gamut. A large color gamut means better color reproducibility. Color gamut can be defined either in CIE 1931 or CIE 1976 color space. Although CIE suggests using CIE 1976 definition since it is a color uniform space, many companies and research groups are still using CIE 1931 to evaluate their products [28]. To satisfy both camps, later we will present color gamut in both CIE 1931 and CIE 1976.

2.2 Backlight, color filters and LC modes

The selection of color filters and light sources plays a crucial role affecting display system efficiency and color performance. Figure 2 depicts the normalized emission spectrum of four backlight sources (CCFL, 1p-LED: WLED with one yellow phosphor, 2p-LED: WLED with red and green phosphors, and RGB LEDs) and the transmission spectra of color filters commonly used for TVs. This set of color filters has peak transmittance at R~650 nm, G~535 nm and B~450 nm. However, significant overlap in the blue-green and red-green filters is found which, in turn, degrades the color saturation. To reduce crosstalk, we should match the backlight emission spectrum with the transmission spectrum of color filters. As shown in Fig. 2(a), the emission spectrum of CCFL has some spikes, but the blue-green and yellow spikes appear in the overlapped regions of the color filters. As a result, the crosstalk limits the color gamut to ~75%. In Fig. 2(b), 1p-LED has a sharp emission peak from blue LED (InGaN) with a narrow full-width half-maximum (FWHM~20 nm). However, the fluorescence emission from YAG:Ce yellow phosphor is fairly broad (FWHM~130 nm). The light source itself does not exhibit separated emission bands for green and red. Thus, the color performance totally

#195594 - $15.00 USD Received 12 Aug 2013; accepted 10 Oct 2013; published 25 Oct 2013

relies on the color filters; it has deficiency to display saturated green and red colors. To overcome this problem, a 2p-LED based on novel β-sialon:Eu (green) and $CaAlSiN_3$:Eu (red) phosphors is developed [13]. As shown in Fig. 2(c), 2p-LED has three differentiable emission bands. These three bands match with the transmission spectra of RGB color filters, but the bandwidth of red and green is still relatively broad (FWHM~60 nm). Finally, RGB LEDs exhibit well-separated bands and narrow FWHM. The red LED (AlInGaP) has emission peak at λ~630 nm and FWHM~22 nm, green LED (InGaN) has emission peak at 530 nm and FWHM~43 nm, and blue LED (InGaN) has a peak wavelength at 460 nm with FWHM~24 nm. Due to narrower bandwidth, the light in the overlapped regions of color filters is greatly reduced. Therefore, it should have the best color performance among the four backlights compared.

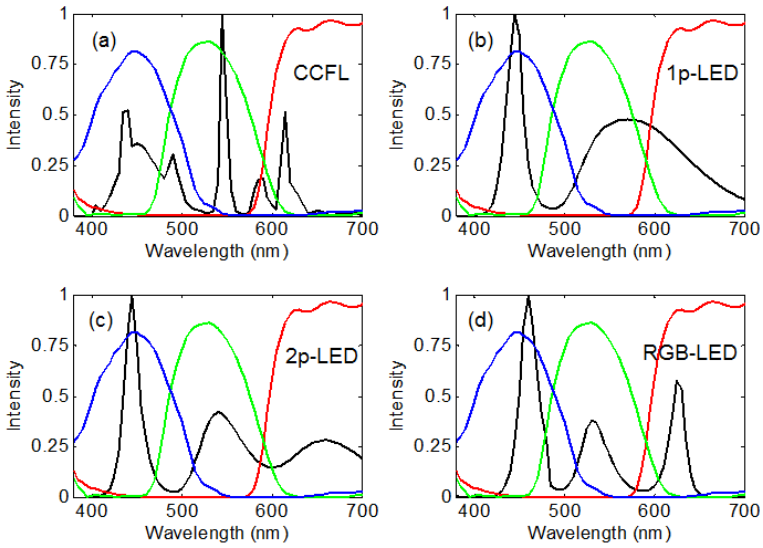

Fig. 2. Normalized emission spectra of four light sources (black curves) and color filters (RGB curves).

To improve simulation accuracy, we also took the transmission spectrum of polarizers into consideration. Figure 3 shows the measured transmission spectra of two linear polarizers in open positions. The transmittance in green and red regions is about 40%, but decreases gradually toward blue. Thus, from the viewpoint of polarizers the selection of blue LED wavelength would affect not only color gamut but also optical efficiency.

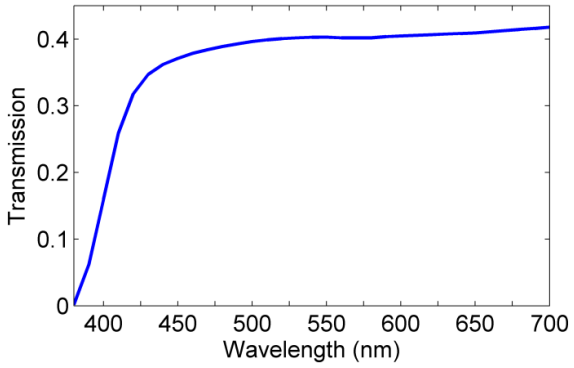

Fig. 3. Transmission spectrum of two open polarizers.

#195594 - $15.00 USD Received 12 Aug 2013; accepted 10 Oct 2013; published 25 Oct 2013

Last but not least, LC mode also plays a key role affecting the color performance and optical efficiency. Here, we calculate the voltage-dependent transmittance (VT) curves of three commonly employed LC modes [29]: twisted nematic (TN) [30] for notebook computers, in-plane-switching (IPS) [31] for mobile displays, and multi-domain vertical alignment (MVA) [32] for TVs. Results are shown in Fig. 4. In each mode, the LC cell is sandwiched between two crossed polarizers. The wavelength dependent absorptions of polarizers and LC birefringence are all taken into consideration during calculation. For TN and IPS, we use a Merck positive dielectric anisotropy (Δε) LC material MLC-6692, whose $\Delta\varepsilon$ = 10.3, Δn = 0.085, and γ_1 = 100 mPas. For MVA, we use Merck negative Δε LC mixture MLC-6608 whose $\Delta\varepsilon$ = –4.2, Δn = 0.083, γ_1 = 186 mPas. The 90° TN has a cell gap d = 5.6 μm. It satisfies the Gooch-Tarry first minimum condition such that $d\Delta n$ = 0.866λ at λ = 550nm [30]. Both MVA and multi-domain IPS cells have same cell gap d = 4 μm and chevron-shaped electrodes in order to obtain wide viewing angle [12].

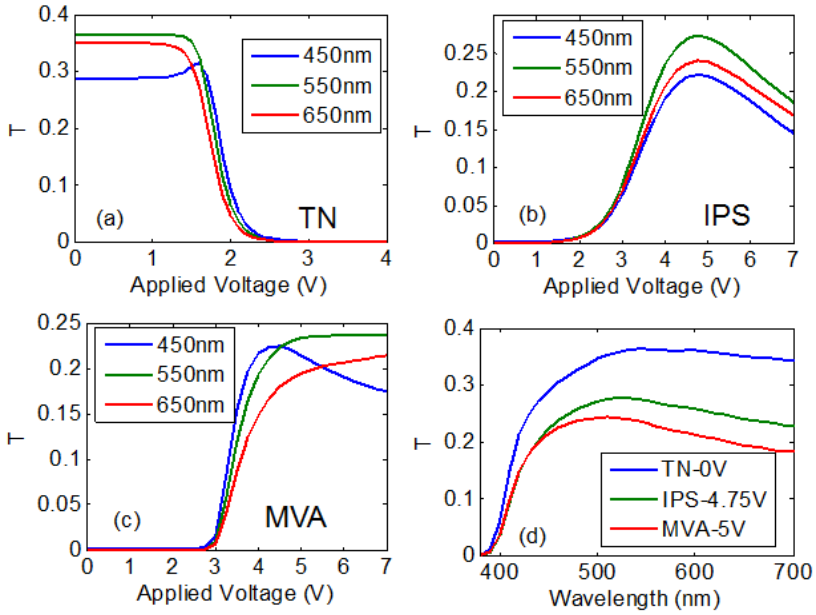

Fig. 4. Simulated VT curves of (a).TN, (b). multi-domain IPS, and (c) MVA cells at R = 650 nm, G = 550 nm and B = 450 nm, and (d). simulated transmission spectra of these three LC modes at the specified voltages.

Figures 4(a)–4(c) show the simulated VT curves of the TN, IPS and MVA cells at three RGB primaries: R = 650 nm, G = 550 nm, and B = 450 nm. The 90° TN cell is normally white, while IPS and MVA are normally black with their peak transmittance at 4.75V and 5V, respectively. However, the phase retardation is dependent on the wavelength and the effective birefringence of the LC layer, thus the VT curves for RGB colors may not overlap and three gamma curves are required for driving the RGB sub-pixels.

Figure 4(d) compares the transmission spectra of TN, IPS and MVA at their corresponding peak voltage. The single domain TN has a higher transmittance than the wide-view MVA and IPS, because multi-domain structures have some domain walls and dead zones that do not transmit light. All these three modes are optimized for the green band (500-550 nm). When λ<450 nm, the absorption from the polarizer plays a significant role and the transmission is reduced considerably. Therefore, the selection of blue wavelength plays an important role affecting the color rendering and overall optical efficiency.

#195594 - $15.00 USD Received 12 Aug 2013; accepted 10 Oct 2013; published 25 Oct 2013

2.3 Evaluation of backlight source

With all the spectral information provided above, we can quantitatively evaluate how a backlight source affects the color performance and optical efficiency of a LCD system through Eqs. (1)–(7). For comparison purpose, we choose D65 (x = 0.312, y = 0.329 in CIE1931 color diagram) as our reference point. D65 is a white light, which is very close to the sunlight and prevalent in most displayed images; it is a representative color for display performance evaluation. After knowing the color coordinates of the targeted white light (x_w,y_w,z_w) and three primary colors (x_i,y_i,z_i |i = r,g,b), the relative proportion of each color component (f_r, f_g, f_b) can be determined by solving the following equations:

$$\left.\begin{aligned} \begin{pmatrix} x_w \\ y_w \\ z_w \end{pmatrix} &= F_r \begin{pmatrix} x_r \\ y_r \\ z_r \end{pmatrix} + F_g \begin{pmatrix} x_g \\ y_g \\ z_g \end{pmatrix} + F_b \begin{pmatrix} x_b \\ y_b \\ z_b \end{pmatrix} \\ z_i &= 1 - x_i - y_i \\ f_i &= \frac{F_i}{F_r + F_g + F_b} \end{aligned}\right\}_{i=r,g,b} . \tag{8}$$

The relative proportion of each color component can be controlled either by the aperture ratio or the different LC transmittance. Here we assume the aperture ratio is already optimized, so that all the LC cells remain at the peak transmittance when displaying the targeted color with fully white. In this case the display system could reach its maximum LE and LER.

Table 1 summarizes the performance of TN LCD with the specified backlights. 1p-LED has the highest LER because its broad emission spectrum is located near 550 nm where human eye is more sensitive. On the contrary, 2p-LED has the lowest LER because its green emission band is far away from 550 nm, thus it makes little contribution to brightness perception. In terms of TE, we find that RGB-LED and 2p-LED are superior because their three separated emission bands match with the color filter transmission bands so that less energy is absorbed. As for TER, 1p-LED and RGB-LED are better than CCFL and 2p-LED. The high TER of 1p-LED results from its high LE, while the high TER of RGB-LED is due to its high TE.

Table 1. Performance of a TN LCD with different light sources.

	LER	TE_{max} (%)	TER_{max} (lm/W)	Color Gamut in CIE1931	Color Gamut in CIE1976
CCFL	301.9	8.7	26.3	77%	98%
1p-LED	319.4	8.7	27.9	75%	97%
2p-LED	254.1	9.4	23.9	89%	115%
RGB-LED	294.7	9.2	27.2	95%	118%

Table 1 also lists the simulated color gamut for the four light sources. While RGB-LED outperforms the other three, its color gamut is 95% in CIE 1931 and 115% in CIE 1976 color space. In general, the color gamut defined by CIE 1976 is much larger than that defined by CIE 1931. To better illustrate and interpret the simulated results, we plot the RGB primaries of the four light sources in CIE 1931 and CIE 1976 color space, respectively, as Figs. 5(a) and 5(b) show. From Fig. 5(a), the green primary of each light source is closer to the center compared to NTSC standard. This is because the green color filter has some crosstalk with red and blue, as Fig. 2 shows. The incident light which aims to display blue/red may also leak to the green channel so that the displayed green color is not pure. As depicted in Figs. 2(a) and 2(b), a portion of CCFL and 1p-LED emission falls into the overlapping regions of the color filters. Therefore, their green primaries move toward the center in the CIE diagram. This green deficiency is the major cause for the reduced color gamut in CIE 1931.

#195594 - $15.00 USD Received 12 Aug 2013; accepted 10 Oct 2013; published 25 Oct 2013

Figure 5(b) shows the RGB primaries in CIE 1976 color space. In contrast to CIE 1931, CIE 1976 has a much smaller area in the green and cyan colors. As a result, the green deficiency is less important in determining the color gamut. Thus, the color gamut defined in CIE1976 is generally larger than that of CIE 1931. CIE 1976 color space is generally regarded as uniform chromaticity diagram and should be more representative to the color performance of a display device. But currently CIE 1931 is still the primary language for major LCD manufacturers to express the color performance of their products [28].

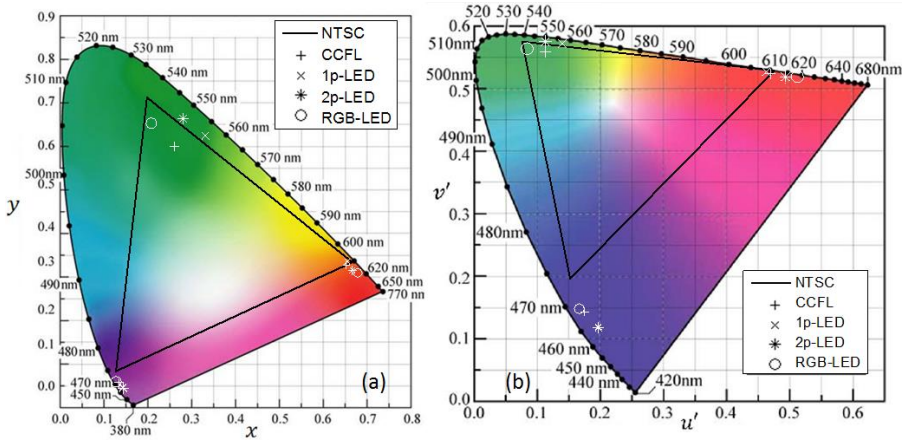

Fig. 5. RGB primaries of different light sources and the NTSC standard primaries in (a) CIE 1931 and (b) CIE 1976. LC mode: TN.

In terms of energy efficiency and color gamut, RGB-LED seems to be the optimal solution, yet it requires complicated driving circuits and its cost is high. From low cost perspective, WLED based on blue LED-pumped phosphorescence is still a favored choice.

3. Spectral optimization of QD backlight

3.1 QD structure and emission spectrum

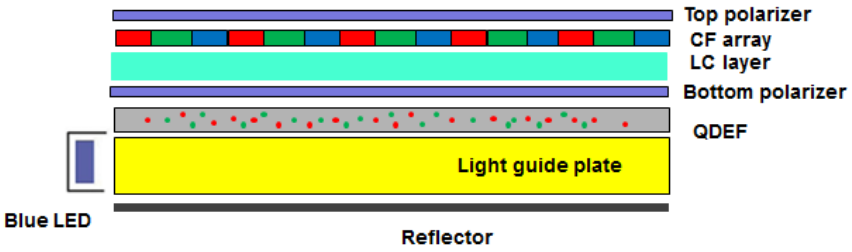

Fig. 6. Schematic diagram of a LCD system with QDEF backlight. The wide-view compensation films are not shown.

Figure 6 is a schematic diagram with a quantum dot enhancement film (QDEF) placed on top of a light guide plate (LPG) [22]. In QDEF, green and red QD nanoparticles are evenly distributed. The edge-lit blue LED array propagates in the LGP and is steered upward to the LCD panel. The emerging blue light from LGP excites the QDs dispersed in the QDEF. Once the excited electrons relax back to their ground states, QDEF emits green and red lights. Together with the transmitted blue light, there are three primary colors (RGB) entering the LCD panel.

In order to use the correct emission spectra in our simulation, we measured the optical performance of two QD samples purchased from Cytodiagnostics. The QD materials have

#195594 - $15.00 USD Received 12 Aug 2013; accepted 10 Oct 2013; published 25 Oct 2013

core-shell structure, with CdS_xSe_{1-x} as core and ZnS as shell. The particle size is between 5.5 nm and 6.5 nm. Due to quantum confinement effect [17], the emission wavelength of QD can be shifted either by varying the QD size or composition. Our QD samples emit color in red or green region by changing the composition ratio *x* of the core material. Figure 7(a) shows the measured absorption spectrum of our green and red QD samples. Both of them exhibit a broadband absorption in the blue region. When excited by a blue InGaN LED (λ = 459 nm), our QD samples emit green and red lights with high purity, as Fig. 7(b) shows. The distribution follows a Gaussian function since it originates from inhomogeneous broadening of QD size and shape distribution. We used Gaussian distribution to fit the measured emission spectrum:

$$f(\lambda) = A \cdot \exp[(\lambda - \lambda_c)^2 / 8\ell n(2)(\Delta\lambda)^2], \tag{9}$$

where A, λ_c and $\Delta\lambda$ are the amplitude, central wavelength and FWHM of the emission band. As shown in Fig. 7(b), the fittings for both green and red QDs are quite good. Through fitting, we find the FWHM of green and red QD emissions is 31.7 nm and 32.2 nm, respectively. QDs have much narrower emission spectra than conventional phosphors (FWHM~50-100 nm). Sharp QD emission spectra lead to vivid colors. Also from experiment, we found that the QD emission intensity is linearly proportional to the pumping intensity. This means the ratios of blue, red and green remain unchanged as the excitation intensity varies, and the displayed color is not affected by the display brightness.

Compared to conventional light sources, QDs offer more spectral design freedom because the central wavelength, FWHM, and emission intensity can be controlled during QDEF fabrication. The central wavelength of green and red colors can be fine-tuned by changing the QD size and composition, and its FWHM can also be controlled by the size distribution. Finally, the emission intensity of RGB colors can be tuned by properly monitoring the green and red QD concentrations and the QDEF thickness. We can take advantage of the design freedom to optimize the color performance for a LCD panel.

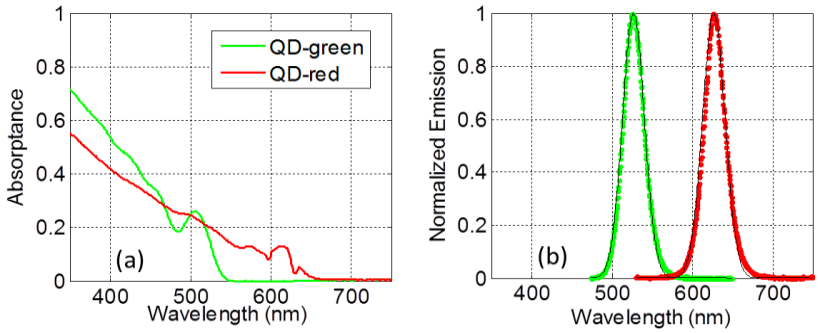

Fig. 7. (a) Measured absorption spectrum of the green and red QDs, and (b) Normalized emission spectrum of green and red QDs when pumped by a blue InGaN LED whose emission peak wavelength is λ = 459 nm.

3.2 Objective function and optimization procedure

After the blue LED light passing through the QDEF, it combines with the emitted red and green beams to form a white light with spectral power distribution $P_{in}(\lambda)$, which can be expressed as:

$$P_{in}(\lambda) = f_b S(\lambda, \lambda_b, \Delta\lambda_b) + f_g S(\lambda, \lambda_g, \Delta\lambda_g) + f_r S(\lambda, \lambda_r, \Delta\lambda_r). \tag{10}$$

In Eq. (10), $S(\lambda, \lambda_b, \Delta\lambda_b)$ represents the blue LED emission spectrum transmitting through the QDEF, while $S(\lambda, \lambda_g, \Delta\lambda_g)$ and $S(\lambda, \lambda_r, \Delta\lambda_r)$ are the emission spectra of the green and red QDs.

#195594 - $15.00 USD Received 12 Aug 2013; accepted 10 Oct 2013; published 25 Oct 2013

λ_i (i = b,g,r) stands for the central wavelength of blue, green and red color components, $\Delta\lambda_i$(i = b,g,r) and f_i(i = b,g,r) are the FWHM and relative proportion of each color component. The emission spectrum of each color component is modeled as Gaussian function. To make a fair comparison with conventional light sources, we also let the LCD panel with QD backlight to display the D65 white light. The relative proportion f_i of three color components can be optimized to display D65. Aperture ratio of each light channel is the same and LC cells in each light channel are all set at the maximum transmittance when displaying the targeted white color. f_i can be solved exactly by Eq. (8). Once f_i is determined and fixed, the remaining free parameters are central wavelength and FWHM for each color component. In total, there are 3x2 = 6 free parameters and two metric functions that are subject to optimization:

$$\begin{aligned} Color\ gamut &= F_1(\lambda_b, \Delta\lambda_b, \lambda_g, \Delta\lambda_g, \lambda_r, \Delta\lambda_r), \\ TER &= F_2(\lambda_b, \Delta\lambda_b, \lambda_g, \Delta\lambda_g, \lambda_r, \Delta\lambda_r). \end{aligned} \tag{11}$$

Most QD samples emit light with FHWM~30-50 nm depending on the size and composition distribution [25]. For practical applications, the following constraints are put on each free parameter: 400 nm < λ_b <500 nm, 500 nm < λ_g < 600 nm, 500 nm < λ_r < 600 nm, 20 nm ≤ $\Delta\lambda_b$ ≤ 30 nm, 30 nm ≤ $\Delta\lambda_g$ ≤50 nm, 30 nm ≤ $\Delta\lambda_r$ ≤50 nm. Optimization is preformed to maximize the above two metric functions within the constrained six dimensional searching space.

For such a multi-objective problem, different objectives may be mutually exclusive. Therefore, a result that simultaneously satisfies each objective may not exist. Instead, a group of solutions could be obtained; any further improvement of the solution in terms of one objective is likely to be compromised by the degradation of another objective. Such solutions constitute a so-called *Pareto front* [33]. Lots of multi-objective global optimization algorithms are available in the literature. In this paper we choose the particle swarm optimization algorithm as optimization solver [34]. It has weak dependence on starting solution and can be conveniently modified for multi-objective problem to find the *Pareto front*. A detailed description of the algorithm can be found in Ref [35].

3.3 Results and discussion

We first performed the optimization for a TN LCD. Since color gamut in Eq. (11) can be defined either in CIE 1931 or CIE 1976 color space, we performed two separate optimizations. Results are plotted in Figs. 8(a) and 8(b). The performance of conventional backlight sources is also included in the same figure for comparison. In Fig. 8(a), the black curve represents the *Pareto front* of QD backlight performance. The QD backlight could vary from low color gamut (77% NTSC) but high TER (32.3 lm/W) to high color gamut (123% NTSC) but low TER (<20 lm/W). The tradeoff between TER and color gamut is obvious because the gain of one metric results from the loss of the other.

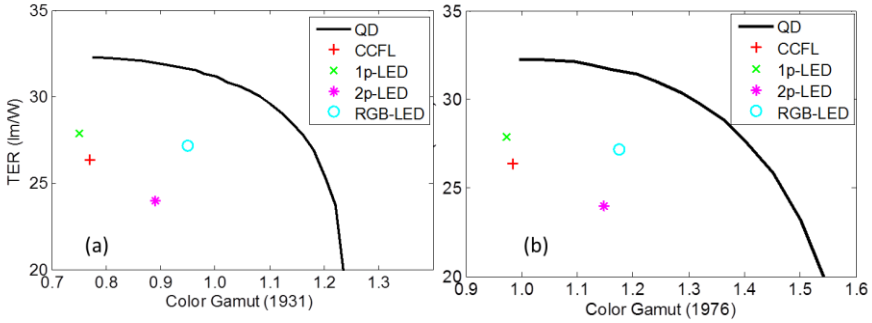

Fig. 8. Relationship between TER and color gamut defined in (a) CIE 1931, and (b) CIE 1976 color space. LC cell: TN mode.

#195594 - $15.00 USD Received 12 Aug 2013; accepted 10 Oct 2013; published 25 Oct 2013

From Fig. 8(a), it is evident that QD backlight has superior performance to conventional backlights. For example, by keeping the same LER as that of RGB-LEDs, the QD backlight can achieve 118% color gamut, which is much larger than that of any conventional backlight. Similarly, by keeping the same color gamut as RGB-LEDs, the QD backlight can achieve TER~31 lm/w, which is ~13% higher than that of RGB LEDs (27.2 lm/w).

Figure 8(b) shows the *Pareto front* for TER and color gamut defined in CIE 1976 color space. In contrast to the CIE 1931 results shown in Fig. 8(a), the color gamut in CIE 1976 is corresponding higher. By keeping the same TER as that of RGB LEDs, the QD backlight can achieve >140% color gamut.

Table 2 lists some optimal QD spectral solutions that have their performance lie on the *Pareto front* line in Fig. 8(a). From QD1 to QD5, the CIE 1931 color gamut gradually increases from 0.8 to 1.2, while TER decreases from 32.2 lm/w to 25.3 lm/w. An interesting finding is that all the QD spectrum solutions have their FWHM approaching the lower limit (20 nm for $\Delta\lambda_b$ and 30 nm for $\Delta\lambda_g$ and $\Delta\lambda_r$). This means a narrow emission spectrum is always preferred for enhancing the color performance of the backlight. From QD1 to QD5, λ_b increases while λ_r decreases, so the three emission peaks become more separated from each other. The well-separated emission bands help expand color gamut since the distance between RGB primaries become larger. On the other hand, this leads to a lower LER as the red and blue emission bands are farther away from 550 nm so that their contribution to the system's brightness is reduced. Therefore, there is a fundamental tradeoff between system efficiency and color gamut. Depending on different application needs and display requirements, we can have different weight ratio on the two performance criteria and pick up a proper solution from the *Pareto front* line. To elaborate this tradeoff further, we choose QD1 and QD5 as an example for comparison.

Table 2. Optimal QD spectrum solutions and their spectral parameters and performance.

QD spectral solution	QD1	QD2	QD3	QD4	QD5	QD6
λ_b (nm)	454.1	452.0	450.1	449.7	447.6	443.2
λ_r (nm)	548.0	542.7	535.6	529.8	523.5	547.1
λ_g (nm)	606.5	611.3	615.0	621.8	634.8	635.7
$\Delta\lambda_b$ (nm)	20.1	20.6	20.1	20.9	20.0	20.0
$\Delta\lambda_r$ (nm)	30.1	30.8	30.4	30.4	30.0	30.0
$\Delta\lambda_g$ (nm)	30.5	30.3	30.3	30.6	30.0	30.0
f_b (%)	48.2	47.1	46.1	42.8	37.3	44.8
f_r (%)	30.8	29.8	28.8	29.3	27.8	30.2
f_g (%)	20.9	23.1	25.1	27.9	34.9	24.9
LER (lm/w)	362.6	348.4	329.7	302.8	249.6	301.3
TE (%)	8.9	9.2	9.4	9.7	10.1	9.2
TER (lm/w)	32.2	31.9	31.1	29.5	25.3	27.8
Color gamut-1931	0.80	0.90	1.00	1.10	1.20	1.01
Color gamut-1976	1.00	1.09	1.16	1.23	1.31	1.40

#195594 - $15.00 USD Received 12 Aug 2013; accepted 10 Oct 2013; published 25 Oct 2013

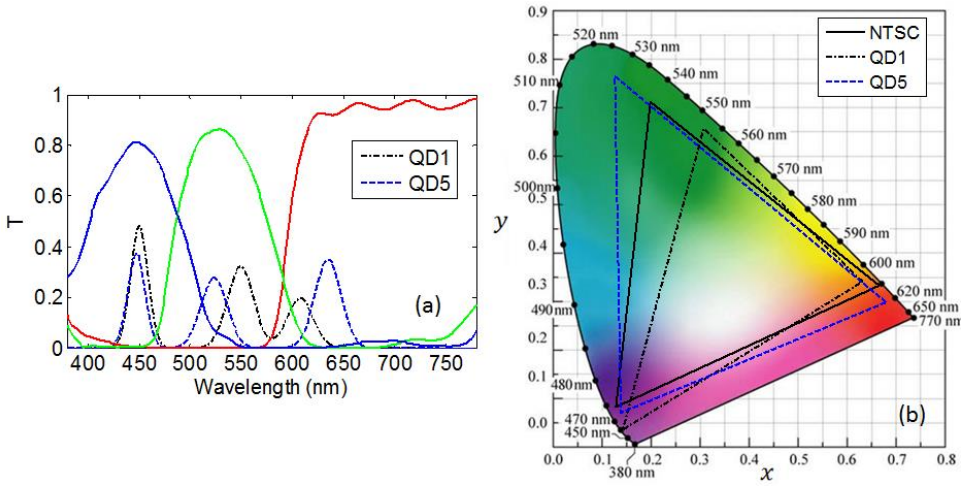

Fig. 9. (a) Transmission spectra of color filters and emission spectra of QD1 and QD5; (b) Simulated color gamut of QD 1 and QD 5 in CIE 1931.

Figure 9 compares the emission spectra and color primaries of QD1 and QD5. In reference to QD1, the three emission bands of QD5 match well with the transmission peaks of color filters. As a result, QD5 has a high TE, but due to low LER, its total system efficiency is still inferior to that of QD1. From Fig. 9(a), only a small portion of QD5 emission spectrum falls into the overlapped blue-green region of the color filters. For example, the red color filter transmits the red emission band while totally blocking the blue and green emissions. This leads to highly saturated RGB color primaries. From the CIE 1931 diagram shown in Fig. 9(b), all the RGB primaries of QD5 are very close to the monochromatic limit. Figure 9(b) also demonstrates that the location of green primary having a significant impact on the color gamut. In order to encircle a large area in the color space, it is desirable to have green emission peak at 520 nm. The conventional green emission band centered at λ = 550 nm is helpful for achieving a high LER, but it leads to a smaller triangle in CIE color diagram.

#195594 - $15.00 USD Received 12 Aug 2013; accepted 10 Oct 2013; published 25 Oct 2013

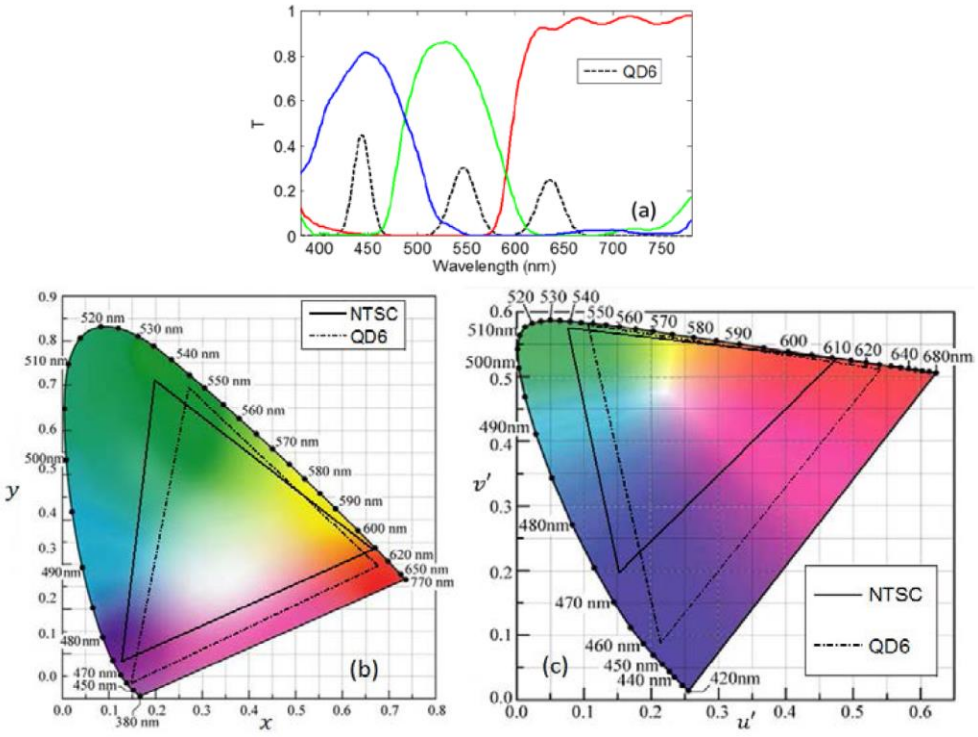

Fig. 10. (a) Transmission spectra of color filters and emission spectrum of QD6, (b) Color primaries of QD6 as well as NTSC standard in CIE 1931 color space, and (c) Color primaries of QD 6 and NTSC standard in CIE 1976 color space

In Table 2, QD1 to QD5 are optimized for CIE 1931 color space, while QD6 is optimized for CIE 1976 color space. QD6 has a very wide color gamut in CIE 1976 color space (140% NTSC), but its color gamut in CIE 1931 is smaller (101% NTSC). Figure 10 depicts the QD6's emission spectrum, as well as its color primaries in different color space. QD6 has its green emission band at 550 nm. Compared to QD5, QD6 has very pure blue primary since only a tiny portion of green emission band leaks through the blue color filter. In CIE 1931 color space, green and cyan colors occupy a very large area, and the color coordinates of green primary affect the color gamut greatly. While in CIE 1976, blue area occupies a large portion and blue color primary plays a more important role. As a result, QD6 has a smaller color gamut in CIE 1931 than that in CIE 1976. The difference between QD5 and QD6 reveals the importance of color space selection when evaluating the color performance of a display device.

Next, we evaluate the QD backlight performance for MVA and IPS LCDs. Figures 11(a) and 11(b) depict the calculated *Pareto front* for MVA and IPS, respectively. When compared to the TN mode shown in Fig. 8(a), we find that the color gamut stays at the same level for different LCD modes, but the system's efficiency varies greatly. TN has much higher system efficiency than MVA and IPS. This is because TN has much higher peak transmittance, while the wide-view MVA and IPS modes employ chevron-shaped electrodes resulting in some transmission dead zones either on top of electrodes or between slits [31, 32]. Figure 11 once again proves that QD outperforms conventional backlights in system efficiency and color gamut for all the three major LCD modes studied.

#195594 - $15.00 USD Received 12 Aug 2013; accepted 10 Oct 2013; published 25 Oct 2013

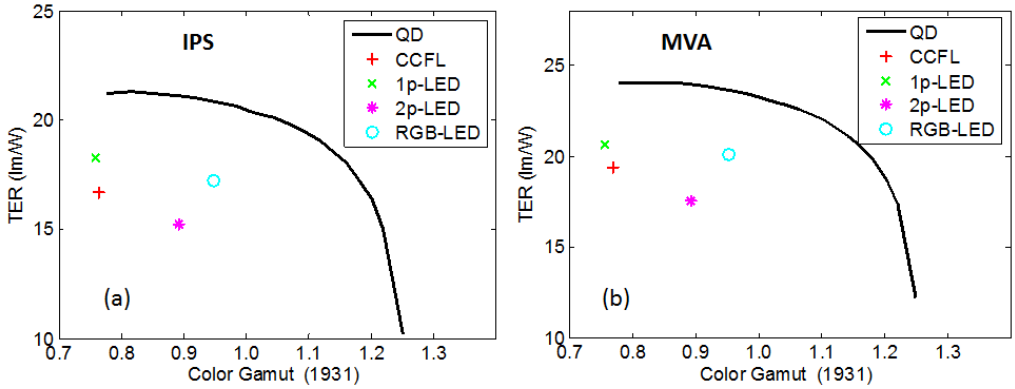

Fig. 11. Relationship between of TER and color gamut for (a) IPS and (b) MVA LCDs.

We also investigated the influence of FWHM on backlight performance. During previous calculations, green and red QD emission bands are assumed to have a lower limit on FWHM, namely $\Delta\lambda_g$ & $\Delta\lambda_r \geq 30$nm. The optimization process can be repeated with increased lower limit of FWHM. Figure 12 is a plot of the simulation results. As the lower limit of $\Delta\lambda_g$ and $\Delta\lambda_r$ increases from 30 nm to 50 nm, both color gamut and TER are reduced. This is understandable since a broader emission band leads to less saturated color primary and narrower color gamut. In order to compensate this effect, the three emission bands should be well-separated, so LER is also reduced. In general, narrower QD emission is always preferred for a high performance backlight.

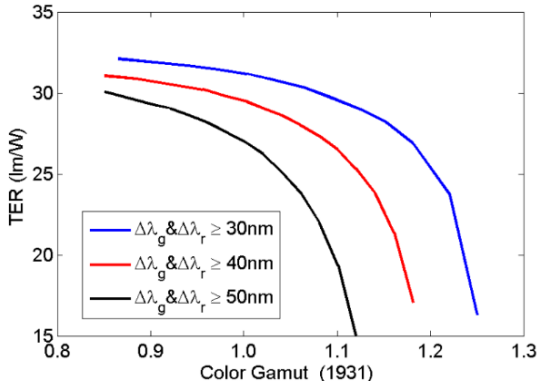

Fig. 12. Simulated *Pareto front* of QD backlight for a TN LCD when the FWHM of green and red emission peak has lower limit of 30 nm, 40 nm and 50 nm.

In addition to FHWM, the variation of central wavelength could also affect the backlight performance. In practical applications the emission wavelengths of QD backlight could deviate from the ideal ones due to manufacturing tolerance. To simulate this effect, we take QD5 listed in Table 2 as an example. It has three emission peaks located at 447.6 nm, 523.5 nm and 634.8 nm. The simulated TER is 25.3 lm/w and color gamut ~120%. We numerically generated 100 random QD spectra by allowing three emission peaks to randomly vary within the range of ± 10 nm from the optimal wavelengths and calculated the performance of the random QD spectrum. On average, the TER could drop to 24.8 lm/W and color gamut to 117%. The effects are not too significant.

Our optimized results indicate that QD backlight has potential to cover color gamut over 120% NTSC in CIE 1931 color space and 140% NTSC in CIE 1976 color space. QD backlight allows LCD to display original colors with high fidelity and make LCD more

#195594 - $15.00 USD Received 12 Aug 2013; accepted 10 Oct 2013; published 25 Oct 2013

competitive as compared to the OLED technology. Moreover, this technique can be conveniently integrated with existing production process and is cost effective. These attractive features guarantee QD display as a promising backlight solution for next generation LCD.

Recently, Samsung [25] and Nanosys [22] reported their products to cover 104.3% and 109% NTSC in CIE 1931 color space. Our simulation results shows there is still room for improvement. The gap between our simulation results and real product's performance may attribute to the control of FWHM and central wavelength of each color component. The spectral distribution of QD emission is mainly affected by the inhomogeneous broadening due to size and shape distributions of QDs, and the central wavelength is mainly influenced by the average size of the QD particles (and also composition). Current synthesis techniques, such as rapid-injection method and continuous flow method, have evolved quickly and enable precise control of QD size and shape [21]. With this synthesis improvement, QD backlight can have an even brighter future.

4. Conclusion

We report a photometry study on QD-based backlights for liquid crystal display. The optimal emission spectrum is obtained by multi-objective optimization method. The fundamental tradeoff between display system's efficiency and color gamut is observed and responsible mechanisms explained. QD backlight outperforms conventional backlight sources in both system efficiency and color gamut. Especially it can reach color gamut of 115% NTSC standard in CIE1931 color space and 140% NTSC in CIE 1976 color space while keeping the same energy efficiency as conventional light sources. Our photometric study proves that QD is a competitive backlight solution and also provides some guidelines for improving QD backlight design.

Acknowledgments

The authors are indebted to Yu-Chieh Lin and Wen-Ching Tsai of AU Optronics (Taiwan) for providing the transmission spectra of color filters, Rongjun Xie of National Institute for Materials Science (Japan) for providing the spectrum of phosphors-based WLED, and Tony Wang of 3M for useful discussion. This work is supported by Industrial Technology Research Institute, Taiwan.

#195594 - $15.00 USD Received 12 Aug 2013; accepted 10 Oct 2013; published 25 Oct 2013